AGU PUBLICATIONS

JGR

Journal of Geophysical Research: Oceans

RESEARCH ARTICLE

10.1002/2016JC012092

Key Points:
- Distinct patterns of variation in photophysiological parameters were evident for different phytoplankton communities
- Patterns of photoacclimation under varying light gradients differed for waters dominated by different phytoplankton groups
- Multiple-regression models for different phytoplankton communities showed promise for estimation of regional photophysiological parameters

Supporting Information:
- Supporting Information S1

Correspondence to:
S. E. Lohrenz,
slohrenz@umassd.edu

Citation:
Chakraborty, S., S. E. Lohrenz, and K. Gundersen (2017), Photophysiological and light absorption properties of phytoplankton communities in the river-dominated margin of the northern Gulf of Mexico, *J. Geophys. Res. Oceans*, *122*, 4922–4938, doi:10.1002/2016JC012092.

Received 24 JUN 2016
Accepted 19 MAY 2017
Accepted article online 24 MAY 2017
Published online 16 JUN 2017

Photophysiological and light absorption properties of phytoplankton communities in the river-dominated margin of the northern Gulf of Mexico

Sumit Chakraborty[1], Steven E. Lohrenz[1], and Kjell Gundersen[2]

[1]School for Marine Science and Technology, University of Massachusetts-Dartmouth, New Bedford, Massachusetts, USA, [2]Institute of Marine Research, Bergen, Norway

Abstract Spatial and temporal variability in photophysiological properties of phytoplankton were examined in relationship to phytoplankton community composition in the river-dominated continental margin of the northern Gulf of Mexico (NGOM). Observations made during five research cruises in the NGOM included phytoplankton photosynthetic and optical properties and associated environmental conditions and phytoplankton community structure. Distinct patterns of spatial and temporal variability in photophysiological parameters were found for waters dominated by different phytoplankton groups. Photophysiological properties for locations associated with dominance by a particular group of phytoplankton showed evidence of photoacclimation as reflected by differences in light absorption and pigment characteristics in relationship to different light environments. The maximum rate of photosynthesis normalized to chlorophyll (P^B_{max}) was significantly higher for communities dominated (>60% biomass) by cyanobacteria + prochlorophyte (cyano + prochl). The initial slope of the photosynthesis-irradiance (P-E) curve normalized to chlorophyll (α^B) was not clearly related to phytoplankton community structure and no significant differences were found in P^B_{max} and α^B between different geographic regions. In contrast, maximum quantum yield of carbon fixation in photosynthesis (Φ_{cmax}) differed significantly between regions and was higher for diatom-dominated communities. Multiple linear regression models, specific for the different phytoplankton communities, using a combination of environmental and bio-optical proxies as predictor variables showed considerable promise for estimation of the photophysiological parameters on a regional scale. Such an approach may be utilized to develop size class-specific or phytoplankton group-specific primary productivity models for the NGOM.

Plain Language Summary This study examined the relationships between phytoplankton community composition and associated optical properties as key factors in explaining the variability of photosynthesis-light relationships in the dynamic and complex continental margin of the northern Gulf of Mexico. Photoacclimation of phytoplankton in different light environments, from the highly turbid Mississippi River delta to relatively oligotrophic offshore waters, was evident and considered to be a factor regulating the efficiency of carbon fixation in photosynthesis. Our findings were unprecedented in revealing significant differences in photosynthetic parameters between the major phytoplankton groups in northern Gulf of Mexico waters. This enabled us to build an empirical model to predict photosynthetic parameters for the major phytoplankton groups across the entire study area. These findings provide a basis for further efforts to apply this approach for wider-scale modeling of primary production in the northern Gulf of Mexico.

1. Introduction

Environmental variability can act at the level of physiology (e.g., photoacclimation and nutritional status) within phytoplankton groups or species as well as through effects on species composition to cause variations in photosynthesis-irradiance (P-E) relationships. Two important parameters that describe the P-E relationship are α^B (mg C (mg Chl)$^{-1}$ h^{-1} (μmol photon m^{-2} s^{-1})$^{-1}$), which is the initial slope of the photosynthesis-irradiance relationship and P^B_{max} ((mg C (mg Chl)$^{-1}$ h^{-1}), which is the maximum photosynthetic rate under light-saturated conditions. Variability in these two parameters occurs due to changes in

phytoplankton physiology and community structure and may contribute to uncertainty in estimates of primary production derived using photosynthesis-irradiance models. Therefore, an understanding of the basis for variations in photophysiological properties of phytoplankton communities is crucial. Relationships between photophysiological properties and phytoplankton community structure have been characterized in different parts of the world ocean [*Cermeno et al*., 2005; *Claustre et al*., 2005; *Hashimoto and Shiomoto*, 2002; *Suggett et al*., 2009; *Uitz et al*., 2008]. In addition to community structure, other key factors that influence photophysiological parameters include environmental variables such as irradiance, temperature, nutrient availability, as well as other biological and ecological factors [e.g., *Sakshaug et al*., 1997; *Behrenfeld et al*., 2002; *Claustre et al*., 2005; *Uitz et al*., 2008; *Xie et al*., 2015].

The NGOM is an optically complex and highly productive continental margin (as high as 400 g C m^{-2} yr^{-1}) [*Lohrenz et al*., 2014; *Heilman and Rabalais*, 2008]. Discharge from both Mississippi and Atchafalaya Rivers strongly influences the distribution of dissolved and particulate material [*D'Sa and DiMarco*, 2009; *D'Sa et al*., 2007], nutrients [*Lehrter et al*., 2013; *Turner et al*., 2007], and the availability and spectral properties of light [*Schaeffer et al*., 2011]. In conjunction with the large environmental gradients, our prior research has demonstrated substantial variations in phytoplankton communities across different water mass types and over seasonal time scales in these continental shelf waters [*Chakraborty and Lohrenz*, 2015]. A recent study [*Zhao and Quigg*, 2015] in a shallow inner shelf region of the NGOM also highlighted the importance of phytoplankton community composition in understanding the diel patterns of photosynthesis and photoacclimation under the complicated light and nutrient conditions.

Primary productivity (PP) is highly variable over space and time, and prior studies in the NGOM [*Sklar and Turner*, 1981; *Lohrenz et al*., 1999; *Lehrter et al*., 2009; *Quigg et al*., 2011] have documented strong relationships of regional PP to physical and meteorological factors that modulate the spatiotemporal changes in freshwater inputs, light, nutrients, temperature, and phytoplankton biomass. Over the years, our understanding of variability in regional PP has improved. However, the photophysiological basis of this regional variability remains poorly understood. Several studies [e.g., *Uitz et al*., 2008, 2010] have shown considerable promise in using phytoplankton size class-specific estimates of photosynthesis-irradiance (P-E) parameters to improve estimates of PP using remote sensing algorithms. However, such phytoplankton size class-specific or group-specific information is limited for the continental margin of the NGOM. An earlier study [*Lohrenz et al*., 1994] in the Mississippi River plume (MRP) observed spatial and temporal differences in the P-E parameters that were partially attributed to variations in river discharge, depth, daily PAR, and temperature. That work mainly considered the variation in P-E parameters due to the environmental conditions without explicitly examining the potential linkages between the composition of the phytoplankton community and the associated P-E parameters.

Here we build on previous studies with the overarching goal of improving our understanding of how variations in photosynthetic properties are related to phytoplankton community composition and associated absorption properties in continental shelf waters of the NGOM. Additionally, we sought to identify patterns of photoacclimation in waters having different dominant phytoplankton groups. Finally, we present an empirical approach for estimation of P-E parameters in the NGOM, specific for the different phytoplankton communities, taking into account the relationships to environmental variables and to bio-optical proxies of phytoplankton size class and pigment composition. Such an approach has the potential to improve regional biogeochemical models [*Fennel et al*., 2011; *Xue et al*., 2013], which are requisite to better understanding of carbon cycling and ecosystem processes in the northern Gulf, and may also lead to improved estimates of primary productivity from remotely sensed data.

2. Materials and Methods

Water samples were collected on board the R/V *Cape Hatteras* for (Gulf Carbon 1–3 and 5) and R/V *Hugh R. Sharp* (Gulf Carbon 4) during five cruises that took place in January, April, July, October 2009, and March 2010. Eight transects were made across the NGOM shelf (Figure 1), occupying contrasting water mass types from freshwater ($S \leq 15$) riverine end members dominated by the Mississippi-Atchafalaya River system to oligotrophic oceanic ($S > 33$) waters. Water samples were collected at each station using 10 L Niskin bottles mounted on a rosette and CTD (SeaBird SBE911 plus) profiling system. Discrete water samples were collected and subsequently filtered for particulate absorption, phytoplankton pigment analysis, nutrients, and

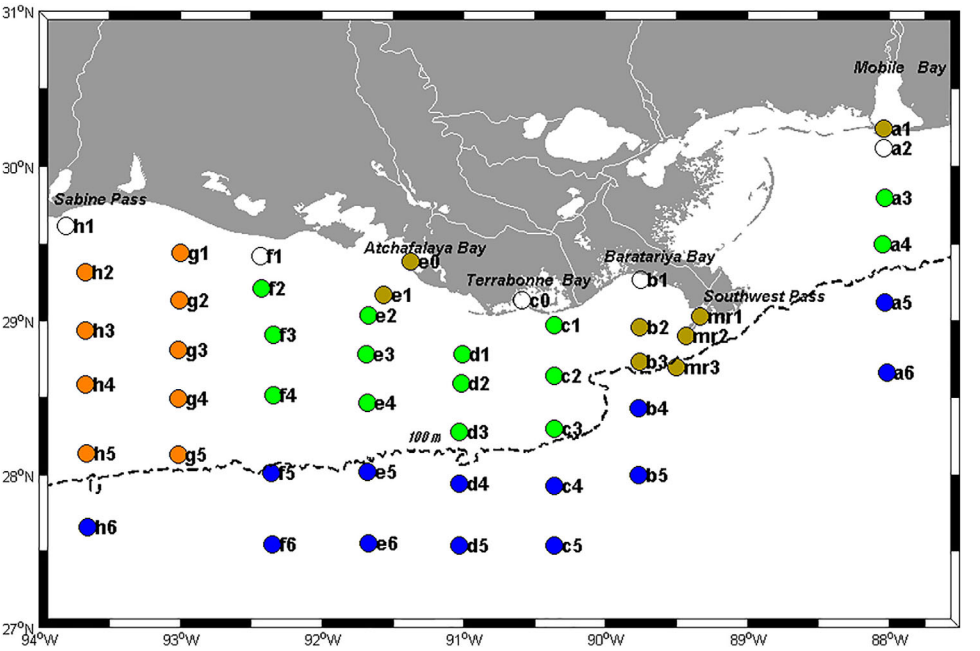

Figure 1. Station locations in the northern Gulf of Mexico. The colored symbols represent the different geographical zones referenced in the text: delta (brown), intermediate (green), far field (orange), and offshore (blue).

P-E experiments. Mixed layer depth (Z_m, m) was determined at each station using the criterion of [*Mitchell and Holm-Hansen*, 1991] as the first depth where the density (sigma-*t*) change over a 5 m interval was $\geq$0.05 kg m^{-3}. Profiles were obtained of hyperspectral downwelling irradiance, E_d (λ, z), in units of W m^{-2} and where λ is wavelength and z is the depth, using a Satlantic HyperPRO free-falling optical profiler equipped with a surface downwelling irradiance (E_s) reference to correct for temporal variability in E_s during profiling. The maximum depth of the optical profiles ranged from a few meters in nearshore waters to 50 m in oligotrophic waters. The value of E_d (λ, z) at just below the sea surface was obtained by extrapolation of logarithm-transformed data from the 1 to 4 m depth interval. Typically, three to five profiles were averaged at a given station. Photosynthetically active radiation (PAR, mol photons m^{-2} d^{-1}) was calculated versus depth by integrating E_d (λ, z) over 400–700 nm. The attenuation of PAR in the water column, K_d (PAR), m^{-1}, was determined as the slope of the least squares regression fit to logarithm-transformed E_d (PAR) as a function of depth. Following *Lehrter et al*. [2009], we chose the depth of the euphotic zone (Z_{eu}) as the depth at which PAR had decreased to 1% of the surface value,

$$Z_{eu} = \frac{\ln(0.01)}{-K_d}.$$

2.1. Photosynthesis-Irradiance Curve Measurements

Photosynthesis versus irradiance (P-E) curves were determined from ^{14}C-HCO_3 in vitro incubations similar to that described by *Lewis and Smith* [1983] and *Lohrenz et al*. [1994]. Eighteen 10 mL subsamples with a final specific activity of approximately 1 μCi mL^{-1} were incubated at 0.03–10 mol quanta m^{-2} h^{-1} irradiance and each incubation was terminated by filtration after 0.5 h followed by treatment of the filters with 200 μL 0.1 N HCl to eliminate residual inorganic ^{14}C. Samples for dissolved inorganic carbon (DIC) and chlorophyll *a* (chl *a*) analyses were collected in conjunction with the P-E samples and used to estimate the chlorophyll-specific rate of carbon fixation. The observed P-E relationships were fitted to a mathematical expression [*Platt et al*., 1980], which was chosen because it was found to perform well in representing patterns in the data. Derived parameters included the initial slope of the light-saturated curve (α^B, g C (g chl *a* h)$^{-1}$ (μmol photons m^{-2} s^{-1})$^{-1}$), the specific photosynthetic rate at optimal light (P^B_{max}, mg C mg chl a^{-1} h^{-1}), maximum potential light-saturated photosynthetic rate (P^B_S), and the rate of photoinhibition (β^B, g C (g chl *a* h)$^{-1}$ (μmol photons m^{-2} s^{-1})$^{-1}$). From these parameters, we estimated the light saturation index ($E_k = P^B_{max}/\alpha^B$, mol C (mol photons)$^{-1}$), which is considered the threshold for light limitation of photosynthesis [*Platt et al*., 1980]. Notation for optical variables and photosynthetic parameters is given in Table 1.

Table 1. Description of the Optical and Photosynthetic Parameters Used in the Study

Abbrev.	Definitions	Units
Photosynthetic Parameters		
P^B_{max}	Chlorophyll *a* specific maximum photosynthetic rate	mg C mg chl a^{-1} h^{-1}
α^B	Chlorophyll *a* specific initial slope of the P-E curve	mg C(mg chl *a* h)$^{-1}$ (μmol photons m^{-2} s^{-1})$^{-1}$)
E_k	Light saturation index	μmol photons m^{-2} s^{-1}
Φ_{cmax}	Maximum quantum yield of carbon fixation	mol C(mol photons)$^{-1}$
PP	Primary productivity at the surface	mg C m^{-2} d^{-1}
Bio-Optical Variables		
chl *a*	Concentration of chlorophyll *a*	mg m^{-3}
a_{ph}	Absorption coefficient of phytoplankton	m^{-1}
a^*_{ph}	Chlorophyll *a* specific absorption of phytoplankton	m^2 mg chl a^{-1}
a_{ph}_slope	Normalized spectral slope of the a_{ph} between 488 and 532 nm	Dimensionless
$a_{ph}(440) : a_{ph}(676)$	Absorption ratio of phytoplankton at blue and red	Dimensionless
PPC:PSC	Photoprotective and photosynthetic carotenoids ratio	Dimensionless
$\bar{a}^*_{ph}$	Mean chl *a* specific absorption coefficient of phytoplankton	m^2 mg chl a^{-1}
K_d	Light attenuation coefficient for downwelling irradiance	m^{-1}
Z_{eu}	Euphotic depth	*M*

2.2. Phytoplankton Absorption

The sampling and analysis of particulate absorption ($a_p(\lambda)$, m^{-1}) was measured with a bench top spectrophotometer (Varian Cary 300 UV-Vis) using the quantitative filter pad technique of *Lohrenz et al*. [2003]. Seawater of volume 0.2–2.5 L depending on the amount of particulate material present in the sample was filtered onto a 25 mm Whatman GF/F glass-fiber filter under low vacuum. Immediately following filtration, the filters were stored in liquid N_2 until laboratory analysis. The spectrophotometer was equipped with a 60 mm (diameter) integrating sphere. Filters were placed at the entrance of the sphere and spectral values of absorption coefficients were measured every 0.2 nm between 300 and 800 nm. Following the measurements of $a_p(\lambda)$, absorption coefficients of nonalgal particulates ($a_{NAP}(\lambda)$) were determined by removing pigments using a hot methanol extraction for 30 min followed by rinsing with Milli-Q water to ensure removal of the biliproteins and any excess methanol and finally rinsing with filtered (0.2 μm) seawater. Correction of path length amplification was made according to *Lohrenz* [2000]. Final estimates were made on all spectra after subtracting the mean absorption values between 750 and 800 nm as a baseline correction. Phytoplankton absorption coefficients ($a_{ph}(\lambda)$) were determined as $a_{ph}(\lambda) = a_p(\lambda) - a_{NAP}(\lambda)$. Chl *a* specific phytoplankton absorption ($a^*_{ph}(\lambda)$, m^2 mg chl a^{-1}) was obtained by normalizing $a_{ph}(\lambda)$ by chl *a* concentrations. The maximum quantum yield of CO_2 fixation was determined using the following equation:

$$\Phi_{cmax} = 12,000\alpha^B \left[\frac{\int_{400}^{700} a_{ph}(\lambda) d\lambda}{\int_{400}^{700} d\lambda} \right]^{-1},$$

where 12,000 is the molar weight (mg) of carbon and α^B is the light-limited slope of the P-E curve, normalized to chl *a*. In addition, a normalized spectral slope of the a*ph* spectrum between 488 and 532 nm was determined following the approach of *Eisner et al*. [2003]:

$$a_{ph}\text{\_slope} = \left[a_{ph}(488) - a_{ph}(532)\right] \times \left[a_{ph}(676)(488–532)\right]^{-1}.$$

The a_{ph}_slope was used to examine the relationships of photoprotective pigments to the shape of the phytoplankton absorption in the blue-green spectral region and served as a proxy for photoacclimation and/or changes in pigment composition [*Eisner et al*., 2003].

2.3. Pigment Analyses

For pigment analyses, seawater samples with volume ranging from 0.15 to 1.5 L at the shallow estuarine end member station to 2–5 L at the deep offshore slope waters were filtered through 47 mm Whatman GF/F glass-fiber filters. Filters were immediately frozen and stored in liquid N_2 until analysis. The details of the HPLC analyses are described in *Chakraborty and Lohrenz* [2015]. The pigment data were further organized into the two categories of accessory pigments: (i) photosynthetic carotenoids or PSC—the sum of fucoxanthin, peridinin, 19′-hexanoyloxyfucoxanthin, and 19′-butanoyloxyfucoxanthin and (ii) photoprotective carotenoids or PPC—the sum of zeaxanthin, diadinoxanthin, alloxanthin, and β-carotene. CHEMTAX software v

1.95 [*Mackey et al*., 1996; *Roy et al*., 2011] was used to determine the relative contributions of phytoplankton groups to chl *a*. The CHEMTAX-derived phytoplankton community data set was also separated into three dominant phytoplankton groups. Stations were given phytoplankton community designations as (1) diatom dominated, when the relative percentage of diatoms was $\geq$60%, (2) as cyanobacteria and prochlorophyte (cyano + prochl) dominated, or (3) as mixed groups, when neither diatoms nor cyano + prochl were dominant. Major contributors to the mixed group were chlorophytes, cryptophytes, and haptophytes. Chlorophytes and cryptophytes were particularly abundant in stations near the delta and shallow inner shelf waters while haptophytes were generally more abundant in areas away from the direct influence of the river discharge and in offshore waters [see *Chakraborty and Lohrenz*, 2015]. These operational designations provide a context for examining the bio-optical and photophysiological properties of the phytoplankton communities.

2.4. Measurements of Suspended Particulate Matter (SPM)

Seawater samples were collected by draining an entire Niskin bottle into a 20 L carboy. Prior to withdrawing samples for filtration, the carboy was agitated to ensure uniform distribution of sample. Water samples of 0.05–3.5 L were filtered onto pretared, 0.45 μm pore size, 45 mm diameter Poretics polycarbonate membrane filters. Filtered samples were stored at −20°C in a small plastic petri dish until returning to the lab. Samples were dried for 24 h at 60°C and weighed on a Lettler Precision Analytical Balance. This was repeated over 3–4 days until weight was stable.

2.5. Colored Dissolved Organic Matter (CDOM) Absorption Measurements

Seawater samples were filtered under low vacuum through 0.22 μm polycarbonate filters prerinsed with 50 mL Milli-Q water. The filtrate was immediately stored at 4°C in acid cleaned and Milli-Q water rinsed 250 mL amber glass (Teflon-capped) bottles. Prior to analysis, the samples were allowed to come to room temperature to reduce the chance of any bias occurring due to temperature difference between the sample and the Milli-Q water reference. CDOM absorbance of the filtered water was measured at 1 nm intervals from 250 to 800 nm in a 10 cm quartz cuvette using a bench top spectrophotometer (Cary 300). A baseline correction was made by subtracting the mean absorbance between 650 and 680 nm from the spectrum to remove instrument baseline drift and refractive effects. The measured absorbance (A [λ]) values were converted into absorption coefficients, $a_{CDOM}(\lambda)$ (m^{-1}) according to the following:

$$a_{CDOM}(\lambda) = \frac{2.203.\ A(\lambda)}{l},$$

where *l* was the path length of the cuvette. The spectral slope (SCDOM) for each spectrum was calculated by applying a nonlinear, least squares fit to the measured $a_{CDOM}(\lambda)$ values between 350 and 500 nm [*Babin et al*., 2003]. The fit was performed using the raw (i.e., nonlog-transformed) data [*Twardowski et al*., 2004]:

$$a_{CDOM}(\lambda) = a_{CDOM}\ (\lambda_r) e^{(-S_{CDOM}(\lambda-\lambda_r))}.$$

2.6. Nutrients

Samples for nutrients were initially filtered through Whatman 25 mm GF/F filters and refrigerated in acid-washed, polyethylene bottles until analysis on shore. Nutrient samples were analyzed for nitrate (NO_3), nitrite (NO_2), ammonium (NH_4), silicate (SiO_3), and phosphate (PO_4). Fluorometric methods were used for nitrogen species and spectrophotometric methods for PO_4 and SiO_3. All nutrient analyses were performed using an Astoria−Pacific A2 + 2 nutrient auto-analyzer (methods #A179, A027, A205, and A221; Astoria Pacific International).

2.7. Statistics

Statistical analyses were conducted using SPSS v24 software. Relationships between P-E parameters and environmental, biological, and optical variables were examined using Spearman correlation coefficients (*r*). The significance of *r* was evaluated with the two-sample *t* test for correlation (Table 2). Kolmogorov-Smirnov and Shapiro-Wilk tests were employed to test the normality of the distribution for each of the variables. Data were log-transformed prior to statistical analyses according to *Campbell* [1995]. In the case of nonnormal distributions, the nonparametric Kruskal-Wallis test was used, which is analogous to an ANOVA.

Table 2. Spearman Correlations of Photophysiological Parameters With Environmental, Phytoplankton Group, and Bio-Optical Properties[a]

Variables	P^B_{max} mg C mg chl a^{-1} h^{-1} (n = 61)	α^B mg C (mg chl a h)$^{-1}$ (μmol photons m^{-2} s^{-1})$^{-1}$) (n = 61)	Φ_{cmax} mol C (mol photons)$^{-1}$ (n = 61)	E_k μmol photons m^{-2} s^{-1} (n = 61)
Environmental				
S	**0.36832**	0.0282	−0.47995	0.15331
T	**0.48063**	−0.00127	−0.40367	0.46675
chl *a*	**–0.50367**	−0.03078	**0.62911**	**–0.35847**
DIN	−0.0934	0.19454	**0.45014**	−0.09574
SiO_3	−0.17995	0.07062	0.36895	−0.31064
PO_4	0.08887	0.04151	0.2565	−0.02997
MLD	**0.25735**	0.16037	**–0.33889**	−0.11338
Z_{eu}	**0.46032**	−0.04232	**–0.5837**	**0.419**
K_d	**–0.43546**	0.03451	**0.58027**	**–0.39167**
SPM	**–0.32953**	0.16078	0.42075	−0.34174
Phytoplankton Groups				
Diatoms	**–0.40223**	**0.06592**	**0.57327**	**–0.39264**
Cyano + prochl	**0.54394**	−0.09779	**–0.53338**	**0.54899**
Mixed	**–0.29335**	0.22789	0.11593	**–0.49177**
Optical Properties				
a_{ph}(440):a_{ph}(676)	**0.54511**	−0.05787	**–0.39473**	**0.44004**
a_{ph} (440)	**0.55732**	0.20791	**–0.41729**	**0.29567**
a_{ph} (676)	**0.66795**	**0.39447**	**–0.31591**	0.20921
a_{ph}_slope	**–0.51891**	0.10563	**0.54592**	**–0.41989**
a_{NAP}(440)	−0.14928	0.30768	0.40401	**–0.36396**
a_{CDOM} (412)	−0.32436	−0.0896	0.41436	**–0.25571**

[a]Bold values indicate significant relationships (i.e., p value < 0.05).

To account for the optical complexity in NGOM and the influence of the large rivers (Mississippi and the Atchafalaya Rivers) on photophysiology and bio-optical properties, four geographical zones (delta, intermediate, far field, and offshore, Figure 1) were identified using hierarchal cluster analysis (HCA). The HCA was carried out using SPSS v.24 software. City block distances were calculated using Ward's minimum variance method. The variables used for the classification of the regions were *T*, *S*, chl *a*, a_{ph}(440), K_d, Z_{eu}, SPM, a_{cDOM}(412), and a_{NAP}(440) (supporting information Figure S1). HCA yielded four major groups and they were similar to the geographical zones identified by several recent studies [*Fennel et al*., 2011; *Laurent et al*., 2013; *Xue et al*., 2013] in the region. The term "geographical zones" refers to the different water types based on their different physicochemical and optical properties and that corresponded to different locations along the shelf.

Differences in P-E parameters between different geographical regions were assessed using nonparametric Kruskal-Wallis ANOVA. The associations between environmental and bio-optical predictor variables and P-E response variables were analyzed using multiple-regression analysis. A stepwise multiple linear regression was used to determine a subset of variables that explained the largest amount of variation in the P-E parameters using a significance cutoff of $p < 0.05$. From this, we selected key factors for the regression (Table 3a). The assumption of independence of error of the multiple linear regressions was verified using the Durbin-Watson statistic and the statistical significance of the model was assessed using the *F*-ratio. The assumption of multicollinearity of variables used in the model and homoscedasticity of errors was also evaluated. Multicollinearity of variables was tested using the variance inflation factor. Homoscedasticity of error

Table 3a. Coefficients of the Stepwise Multiple Regression for P^B_m[a]

Groups (Phytoplankton)	Intercept	Temperature (°C)	a_{ph}(676) (m−1)	$a_{ph}(440) : a_{ph}(676)$	a_{ph}_slope	RMSE	APD
Diatom	4.961	−0.076	461.24	−1.39	52.683	1.5	8.39
Mixed	−4.160	0.165	140.199	2.975	−20.743	2.65	49.05
Cyano + prochl	−0.676	0.291	40.016	2.124	124.211	1.39	4.99
All data	−3.735	0.288	141.08	1.637	73.035	2.55	26.89

[a]Predictor variables included temperature, a_{ph}(676), $a_{ph}(440) : a_{ph}(676)$, and a_{ph_s}lope (RMSE = root-mean-square error; APD = absolute percentage difference).

Table 3b. Coefficients of the Stepwise Multiple Regression for α^B (DIN = Dissolved Inorganic Nitrogen)

Groups (Phytoplankton)	Intercept	DIN q (μM)	$a_{ph}(676)$ (m−1)	$a_{ph}(440) : a_{ph}(676)$	RMSE	APD
Diatom	−0.005	0.002	0.858	0.010	0.007	10.64
Mixed	0.008	0.002	0.746	−0.002	0.009	23.66
Cyano + prochl	−0.010	0.002	2.081	−0.001	0.008	5.23
All data	0.011	0.001	0.755	−0.001	0.008	15.43

distributions was assessed by plotting the standardized residuals of the regression against the unstandardized predictor variables.

3. Results

3.1. Regional Environmental Conditions

Here we briefly summarize the environmental and optical properties of the geographic zones during the study, and subsequently describe the relationship between phytoplankton, light absorption properties, photophysiology, and community composition. Detailed descriptions of the regional variability of optical and environmental properties and their relationship with the phytoplankton community are given elsewhere [*Chakraborty*, 2013; *Chakraborty and Lohrenz*, 2015].

As expected, the delta and the intermediate zones were directly influenced by the large rivers, characterized by low salinity waters (overall mean salinity of 25.8 ± 7.1 standard deviation). Seawater temperatures were relatively high during summer and water columns were highly stratified, while lower temperatures and vertically mixed conditions prevailed during winter 2009 and spring 2010 (supporting information Table S1). Highest mean (0.58 ± 0.25 m^{-1}) light attenuation coefficients (K_d) and shallowest euphotic depths (Z_{eu}) (10.85 ± 6.66 m) were observed during spring 2010. Average values of SPM, $a_{NAP}(440)$, and $a_{CDOM}(412)$ were significantly higher ($p < 0.05$) in the delta and intermediate waters than the far-field and the offshore waters. SPM, $a_{NAP}(440)$, and $a_{CDOM}(412)$ values exhibited significant relationships with salinity (ANOVA, $p < 0.05$, not shown), decreasing with increasing salinity away from the direct influence of rivers. Variations of dissolved nutrients were strongly correlated with river discharge (not shown).

In the far-field zone, away from the direct influence of the rivers and associated freshwater inputs, we observed smaller amplitude in the seasonal variation in the environmental properties. Average salinity (34.7 ± 1.56) in far field was much higher than the delta and intermediate zones, with the exception of spring 2010 (31.04 ± 2.98), when high river discharge (supporting information Figure S2) and strong winds out of the northwest resulted in an extended river plume [*Huang et al*., 2013; *Chakraborty and Lohrenz*, 2015]. Average values of SPM and CDOM and nonalgal particulate absorption were much lower in the far field than observed in the delta and intermediate zones (supporting information Table S1), and as a result light availability was much higher in the far-field zone. K_d was significantly lower (K-S test, $p < 0.05$), while Z_{eu} was significantly higher (K-S test, $p < 0.05$) than observed in the delta and intermediate zones. Average nutrient concentrations were also low (supporting information Table S1).

Over the continental slope of the NGOM, the offshore zone had oligotrophic characteristics. Typical salinity was 36.07 ± 0.95 and nutrient concentrations were generally low; however, atypically low salinities and relatively high nutrient concentrations were observed during spring 2010 (34.2 ± 2.48) and in summer 2009 (<31), which coincided with offshore extension of the river plume as previously described in other studies [*Feng et al*., 2012]. Spring 2010 was also a period of unusually low temperatures, ~2–3°C lower when compared to means from 2002 and 2011 [*Huang et al*., 2013].

3.2. Variability in Phytoplankton Light Absorption, Community Composition, Size, and Pigments

The chlorophyll-specific phytoplankton absorption ($a^*_{ph}(\lambda)$) varied on both seasonal and spatial scales (Figure 2a), a pattern seen in numerous studies [*Bricaud and Stramski*, 1990; *Bricaud et al*., 2004]. The $a^*_{ph}(\lambda)$ spectra had characteristic absorption maxima at 440 and 676 nm and varied by orders of magnitude across different zones (Figure 2a). The CHEMTAX-derived phytoplankton diatom group generally dominated the delta and intermediate areas (>60% of total chl *a*). However, significant (Kruskal-Wallis, $p < 0.05$) seasonal differences were observed during summer and fall when the community was dominated by cyanobacteria + prochlorophyte (cyano + prochl) and other phytoplankton groups [*Chakraborty and Lohrenz*, 2015]. Relative

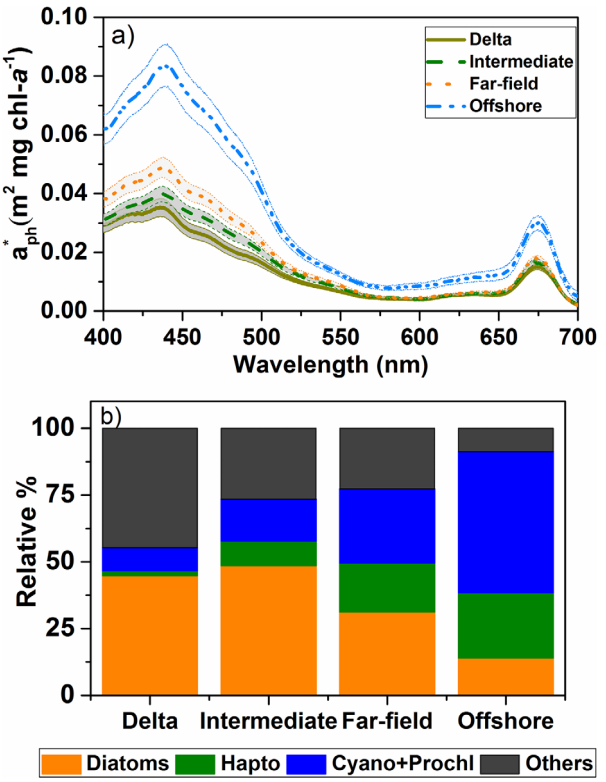

Figure 2. (a) Chlorophyll *a* specific absorption spectra of phytoplankton in each geographic zone. The bold lines represent the means and shaded bands are the standard errors of the means. (b) Relative percentages of chlorophyll *a* as determined using CHEMTAX attributed to major phytoplankton groups. The "Others" group includes the sum of chlorophytes + cryptophytes + prasinophytes + pelagophytes, and the "Hapto" group represents the sum of haptophyte 6 + haptophyte 8. The mixed community referenced in the text is the summation of "Hapto" and "Others" [see *Chakraborty and Lohrenz*, 2015].

proportions of cyano + prochl were systematically higher in offshore waters (Figure 2b), with highest chl *a* proportions observed during spring and fall 2009 (50 ± 15.4%). In contrast, their relative contribution to chl *a* in the offshore waters was exceptionally low (ranged 1.9–8.7%) in spring 2010. Such low abundance of cyano + prochl during spring 2010 in offshore waters was attributed to the offshore extension of a river plume feature as previously discussed. The high availability of nutrients (due to strong NW and upwelling-favorable winds) [*Huang et al.*, 2013; *Chakraborty*, 2013] resulted in conditions suitable for the proliferation of larger phytoplankton groups [*Chakraborty and Lohrenz*, 2015].

Major differences in bio-optical properties were evident for stations dominated by different phytoplankton groups and among the geographic domains. Concentrations of chl *a* varied over orders of magnitude from high chl *a* delta and intermediate waters (range = 0.36–16 and 0.2–29 mg m^{-3}, respectively, Figure 3a) to low values in far-field and offshore waters (0.2–3.4 and 0.04–3.8 mg m^{-3}, respectively). The mean chl *a* specific absorption of phytoplankton ($\bar{a}^*_{ph}$) was significantly lower ($p < 0.05$, K-S test) in the delta region (Figure 3b), while values increased in far-field and offshore waters and highest values were observed in the offshore region. The cyano + prochl group was consistently associated with significantly higher values of $\bar{a}^*_{ph}$, while for diatoms the values of $\bar{a}^*_{ph}$ ranged lower and the mixed group had intermediate values. This pattern was consistent among all the domains (Figure 3). The ratio of $a_{ph}(440)$:$a_{ph}(676)$ was low (median = 2.19, Figure 3c) in the delta and intermediate zones generally dominated by diatoms and other larger groups, while higher $a_{ph}(440)$:$a_{ph}(676)$ values (range = 1.8–4.57, median 2.9, Figure 3c) were associated with far-field and offshore areas where smaller phytoplankton (mainly cyanobacteria and prochlorophytes) dominated. Values of $a_{ph}(440)$:$a_{ph}(676) > 2.5$ can be considered as representing the picophytoplankton group, while $a_{ph}(440)$:$a_{ph}(676)$ values of <2 are indicative of microphytoplankton-dominated communities [*Bricaud et al.*, 2004; *Stramski et al.*, 2001, *Stramski and Morel*, 1990]. Highest values of the normalized slope over 488–532 nm (a_{ph}_slope) were generally found in delta and intermediate zones (Figure 3d). The decrease in a_{ph}_slope (increasingly negative) from delta to offshore waters likely reflected changes in photoacclimation in relationship to higher available irradiance in offshore waters along with associated changes in phytoplankton composition. This was further supported by the finding that a_{ph}_slope varied inversely in relationship to the ratio of PPC:PSC, with decreasing (negative) values of a_{ph}_slope and increasing PPC:PSC from delta to offshore ($p < 0.05$, r = −0.7; supporting information Table S1).

3.3. Variability of P-E Parameters

Differences in surface P^B_{max} values between the different geographical zones were not significant (Figure 4a, $p > 0.05$, K-S test). However, differences in P^B_{max} were observed for stations dominated by different phytoplankton groups (Figure 4a). Average P^B_{max} was ~54% lower at diatom-dominated (>60%) stations relative to cyano + prochl-dominated (>60%) locations. A positive relationship was found between the optical

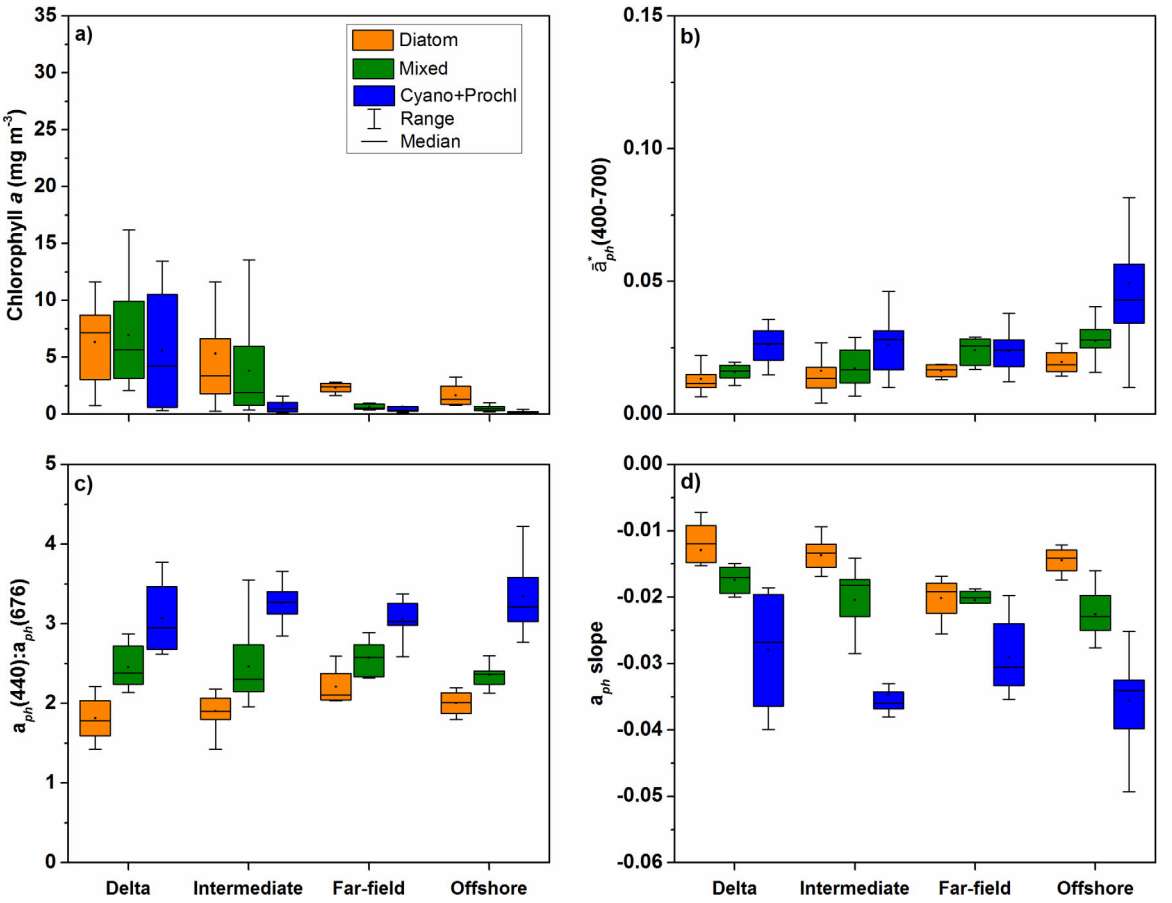

Figure 3. Variability in optical properties among the dominant phytoplankton groups across the different geographic zones, (a) chlorophyll *a*, (b) a^*_{ph} (400–700) (m^2 mg chl a^{-1}), (c) phytoplankton absorption blue to red spectral ratios, $a_{ph}(440) : a_{ph}(676)$, and (d) phytoplankton absorption index of photoacclimation, a_{ph_S} lope.

proxy for phytoplankton size, $a_{ph}(440)$:$a_{ph}(676)$, and P^B_{max} (Figure 5 and Table 2, also see supporting information Figure S3). The relationship of P^B_{max} to the CHEMTAX-derived fraction of chl *a* associated with the diatom group was negative (Table 2), while a positive relationship was seen for cyano + prochl (Table 2). A more complex situation was found for the mixed assemblage group (Table 2 and supporting information Figure S3); both the maximum (25.62 mg C (mg chl *a*)$^{-1}$ h^{-1}) and minimum (2.92 mg C (mg chl *a*)$^{-1}$ h^{-1}) values of P^B_{max} were associated with stations having mixed assemblages.

Significant correlations were found between P^B_{max} and environmental variables (Table 2). Specifically, the correlation was positive with temperature (Figure 5a and Table 2), while relationships to K_d and chl *a* (Figure 5b and Table 2) were negative. No significant relationship was seen for DIN and P^B_{max} (Figure 5c). Highest P^B_{max} values were observed in the midsalinity range (25–32), and a weak positive correlation existed with salinity (Table 2). Values of the initial slope α^B varied widely, over orders of magnitude (range = 0.006–0.103 g C (g chl *a* h)$^{-1}$ (μmol photons m^{-2} s^{-1})$^{-1}$) within the zones (Figure 4b) and among phytoplankton groups and no significant differences were evident. No significant correlations were found between α^B and ambient nutrients, temperature, K_d, and chl *a* (Figures 5d–5f and Table 2).

Unlike P^B_{max} and α^B, the maximum quantum yield of carbon fixation in photosynthesis (Φ_{cmax}) differed significantly (K-S test, $p < 0.05$) between the geographic zones (Figure 4c). Values of Φ_{cmax} decreased along the progression from the river-influenced, light-limited delta to the more oligotrophic waters offshore. Average Φ_{cmax} values in the delta were about 39% greater than that of the offshore waters (Figure 4c and supporting information Table S1). The relative fraction of total chl *a* associated with the diatom group was positively correlated with Φ_{cmax} (Table 2) and the mean Φ_{cmax} for diatom-dominated stations was significantly higher ($p < 0.05$, K-S test) in comparison to the cyano + prochl-dominated communities (Figures 4c and 5g–5i). In general, Φ_{cmax} was significantly correlated with environmental variables (S, T, nutrients, chl *a*, and K_d, Table

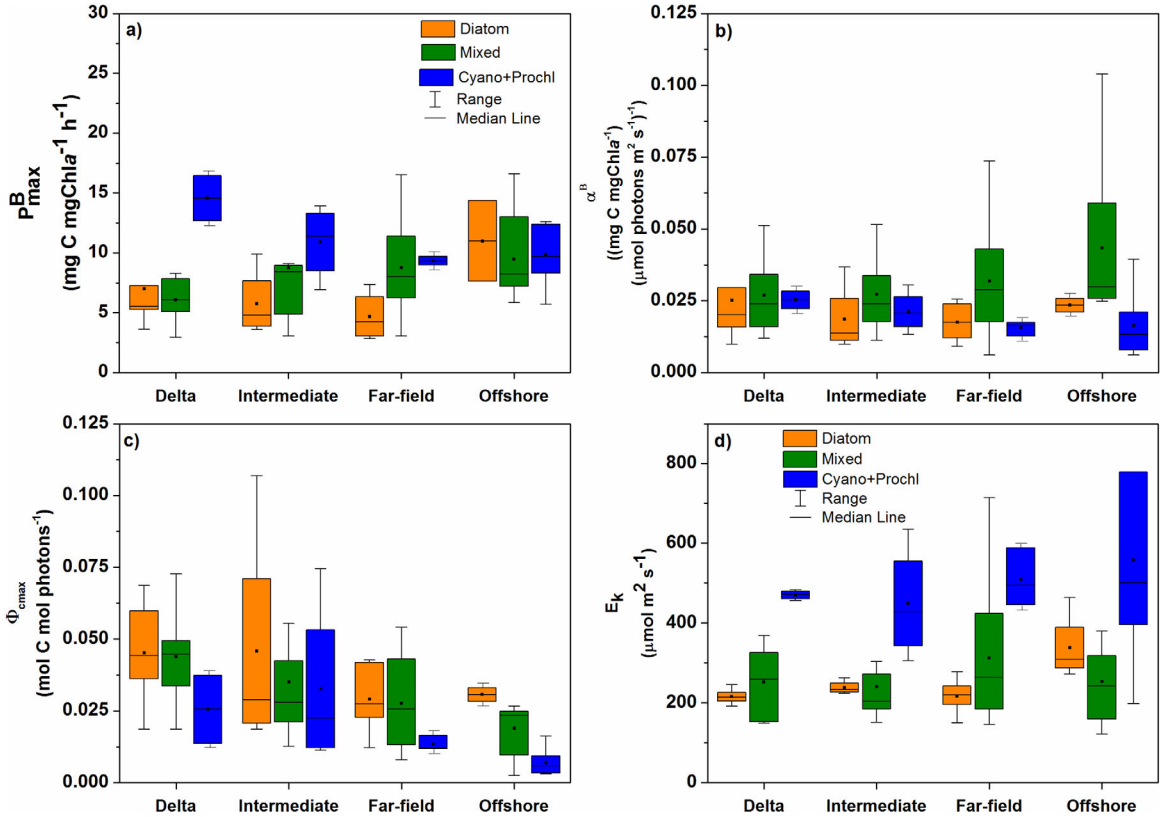

Figure 4. Variability of photosynthetic properties among the dominant phytoplankton groups across geographic zones, (a) maximum photosynthetic rate, P^B_{max}, (b) initial slope of the P-E curve, α^B, (c) maximum quantum yield of carbon fixation, Φ_{cmax}, and (d) light saturation index, E_k.

2). Among the environmental variables, chl *a* and K_d accounted for the greatest percentage of the variation in Φ_{cmax} (Table 2). Furthermore, values of Φ_{cmax} were negatively correlated with blue to red ratios $a_{ph}(440)$:$a_{ph}(676)$ and had a positive relationship to a_{ph}_slope (Table 2).

The light saturation index (E_k) also varied among water masses and phytoplankton groups and photoacclimation state. Significantly higher ($p < 0.05$, K-S test) values of E_k in the cyano + prochl-dominated waters were observed ranging between 197.8 and 779.4 µmol m^{-2} s^{-1} in comparison to a range of 150.0–463.5 µmol m^{-2} s^{-1} for stations dominated by diatoms. The higher values of E_k corresponded with more negative values of a_{ph}_slope (Table 2). E_k was also strongly related to the light environment, with significant correlations observed for Z_{eu} and K_d (Table 2).

4. Discussion

4.1. Factors Regulating Photophysiological Parameters in NGOM: Role of Phytoplankton Community Composition and Environmental Variables

A major focus of this study was to improve understanding of how the variability in P-E parameters was associated with differences in phytoplankton community composition and in relationship to the environmental variables in different geographical zones (delta, intermediate, far field, and offshore, Figure 1). Major differences in P^B_{max} were observed among the dominant phytoplankton groups. Significantly ($p < 0.05$) lower values were observed for diatom-dominated populations than in the mixed and the cyano + prochl-dominated communities, and this pattern was consistent across the different geographic zones. Diatoms, as expected, dominated the high biomass, river-influenced and comparatively low-light deltaic and intermediate zones. The low P^B_{max} and associated low $a_{ph}(440)$:$a_{ph}(676)$ observed in those zones were indicative of increased pigment packaging [*Mitchell-Innes and Walker*, 1991; *Marra et al.*, 2007]. The diatom-dominated communities in low-light environments (high K_d), particularly in the delta and river-influenced intermediate zones, would be expected to exhibit lower carbon:chl *a* ratios and, therefore, have lower P^B_{max}, associated

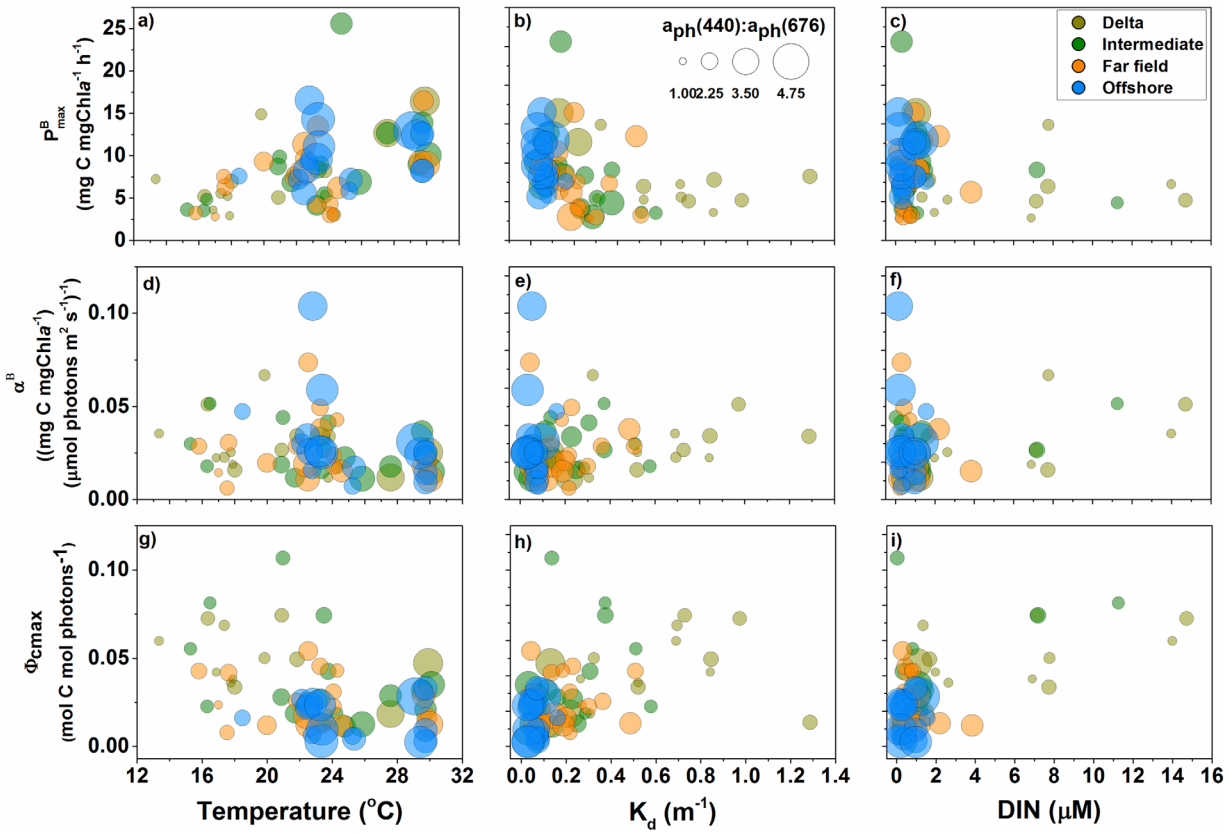

Figure 5. Relationship of P-E parameters with environmental variables (temperature, DIN, and K_d) as a function of $a_{ph}(440) : a_{ph}(676)$ ratios (indicated by symbol size) and geographic zone (indicated by symbol color). The $a_{ph}(440) : a_{ph}(676)$ ratio is used as a proxy for phytoplankton size, for which higher values (larger symbol size) represent small size phytoplankton (e.g., cyanobacteria and prochlorophytes) while the smaller values (small symbol size) correspond to larger phytoplankton such as diatoms.

with low-light acclimation [*MacIntyre et al.*, 2002]. Cyano + prochl communities dominated waters near the delta during summer [*Chakraborty and Lohrenz*, 2015], which could be attributed to the combination of strongly stratified, high-light, and nutrient-limited conditions, that would favor high carbon:chl *a* ratios and hence high P^B_{max} (Figure 4a). The greatest range of variation in P^B_{max} was observed in the mixed phytoplankton group in the far-field and offshore zones. Within the mixed group, haptophytes were a major phytoplankton taxon and are known for their ability to successfully adapt to a wide range of environmental conditions [*Liu et al.*, 2009; *de Vargas et al.*, 2015]. Offshore waters were dominated by the cyano + prochl group. However, P^B_{max} was lower in the cyano + prochl fraction for the offshore waters than that of the cyano + prochl-dominated delta communities. The cyano + prochl in the delta zone, although referred to as cyano + prochl, was mainly composed of *Trichodesmium* and *Synechococcus* and other unicellular cyanobacteria [*Ren*, 2010]. Divinyl chlorophyll *a* (diagnostic pigments for prochlorophytes) was rarely found in our pigment samples from the delta region. The offshore assemblage of cyano + prochl in NGOM was a combination of *Synechococcus* and *Prochlorococcus* [*Chakraborty and Lohrenz*, 2015; *Wawrik and Paul*, 2004], and *Prochlorococcus* has been reported to exhibit lower P^B_{max} and a^*_{ph} than *Synechococcus* [*Shimada et al.*, 1996]. Therefore, the variation of P^B_{max} observed within the delta and offshore cyano + prochl communities was likely a combined effect of physiological differences among taxa as well as differences in environmental conditions.

The significant relationship of P^B_{max} to temperature ($p < 0.05$, Figure 5a) observed in our study was consistent with that of previous work [*Sukenik et al.*, 1987; *MacIntyre and Geider*, 1996; *Bouman et al.*, 2005]. Correlation between P^B_{max} and temperature has been reported numerous times from temperate regions to higher latitudes [*Harrison and Platt*, 1986; *Davison*, 1991; *Sakshaug et al.*, 1997; *Bouman et al.*, 2005]. Significantly higher seawater temperatures were associated with the cyano + prochl-dominated as compared to diatom-dominated communities (K-S test, $p < 0.05$, Figure 5a). *Falkowski and Raven* [1997] reported that increasing

temperatures can stimulate photosynthesis through a direct effect on Calvin cycle enzymatic activity up to an optimal temperature after which rates in photosynthesis can decline due to inactivation and denaturation of enzymes [*Raven and Geider*, 1988]. Observed relationships between P^B_{max} and temperature, particularly in the diatom-dominated stations in our study, were consistent with this concept. Below 21°C, we observed a positive correlation ($r = 0.75$, supporting information Figure S4) between P^B_{max} and temperature for diatom-dominated stations, while P^B_{max} values showed a decline at higher temperatures (>21°C). P^B_{max} was generally negatively correlated with temperature for diatom-dominated stations (Table 2), whereas P^B_{max} and temperature were positively correlated for cyano + prochl-dominated stations. These correlations of temperature with P^B_{max} among the phytoplankton groups may also reflect covariation with other variables. For example, in temperate and subtropical environments, stratification of the water column is mainly temperature driven. In an earlier study [*Chakraborty and Lohrenz*, 2015], it was shown that water temperature, stratification, and mixed layer depths were important environmental factors related to phytoplankton community composition. Highly stratified, low nutrient, and high temperature (i.e., summer) conditions favored picophytoplankton groups, including cyanobacteria and prochlorophytes, while eukaryotic phytoplankton were more prevalent under mixed or less stratified conditions. The correlation of P^B_{max} and temperature can partly be due to the fact that small cells with higher P^B_{max} are typically found in stratified oligotrophic conditions (offshore waters, Figure 5), while larger cells with lower P^B_{max} are dominant during colder periods, when the water column was vertically mixed [*Chakraborty and Lohrenz*, 2015]. The results of this study are in agreement with the assertion of *Platt et al.* [2005] that under light-saturated conditions P^B_{max} is negatively proportional to cell size.

The range of values of P^B_{max} and α^B in the shelf (delta, intermediate, and far field) during this study was similar to that observed by previous studies [*Lohrenz et al.*, 1999; *Lehrter et al.*, 2009, *John et al.*, 2012; *Zhao and Quigg*, 2015]. Variations in α^B showed no apparent relationship to environmental variables, and there was no clear spatial or temporal pattern in observed values. This finding was consistent with that of *Lehrter et al.* [2009]. Their study also did not find significant differences in P^B_{max} and α^B values along the continental shelf of the NGOM for different geographic regions. Higher P^B_{max} associated with smaller phytoplankton has been reported in several previous studies [*Malone and Neale*, 1981; *Côté and Platt*, 1983; *Sathyendranath et al.*, 1999; *Bouman et al.*, 2005]. However, some studies [*Cermeno et al.*, 2005; *Claustre et al.*, 2005; *Uitz et al.*, 2008] have also reported higher P^B_{max} values for larger phytoplankton, such as diatoms, leaving considerable ambiguity in P^B_{max} and phytoplankton size class relationships.

The range of Φ_{cmax} for our study was also consistent with the range for natural algal communities under optimum physiological conditions (0.06–0.08 mol C (mol photon)$^{-1}$) as previously reported [*Bannister*, 1974; *Babin et al.*, 1996]. In contrast to P^B_{max} and α^B, both geographical and taxonomical differences were evident in Φ_{cmax} values. Similar to the findings of this study, high Φ_{cmax} in diatom-dominated populations and other large-sized phytoplankton in low-light (delta zone) environments have been observed elsewhere in the ocean [*Cermeno et al.*, 2005]. *Claustre et al.* [2005] also reported that large phytoplankton composed mainly of diatoms had relatively high Φ_{cmax} in comparison to that for small phytoplankton in the North Atlantic. High pigment packaging in diatoms may result in low $a_{ph}(440)$:$a_{ph}(676)$ and lower a^*_{ph}, which could explain, at least partially, the high Φ_{cmax}. Values of Φ_{cmax} were lower for the smaller phytoplankton groups. The picophytoplankton (generally <2 mm in size), particularly cyanobacteria (e.g., *Synechococcus* and *Trichodesmium*) have been observed to be the predominant picoprokaryotes in the region [*Chakraborty and Lohrenz*, 2015; *Wawrik and Paul*, 2004]. Significant seasonal differences in Φ_{cmax} existed; values of Φ_{cmax} in summer were lower in comparison to other periods (supporting information Table S1), reflecting a combination of changes in community composition, pigment composition, and environmental conditions. DIN:PO_4 values have been shown to be lower in summer in our study region [*Dagg and Breed*, 2003; *Lohrenz et al.*, 2008] (also see supporting information Table S1 for nutrient concentrations), leading to speculation that nutrient limitation [*Dortch and Whitledge*, 1992; *Justic et al.*, 1995] may be a factor in the lower observed Φ_{cmax}. Other reasons for the lower Φ_{cmax} could be attributed to the relative increase of nonphotosynthetic (photoprotective) pigments such as zeaxanthin [*Chakraborty and Lohrenz*, 2015]. Zeaxanthin is a diagnostic pigment for cyanobacteria and it along with other photoprotective pigments are associated with the cell wall [*Fujuta et al.*, 1994] and contribute to the absorption of PAR, but dissipate the absorbed excitation energy rather than transferring it to the photosynthetic apparatus [*Falkowski and Raven*, 1997]. High PPC:PSC ratios during summer [*Chakraborty and Lohrenz*, 2015] would result in a depression of Φ_{cmax} [*Babin et al.*, 1996] and could

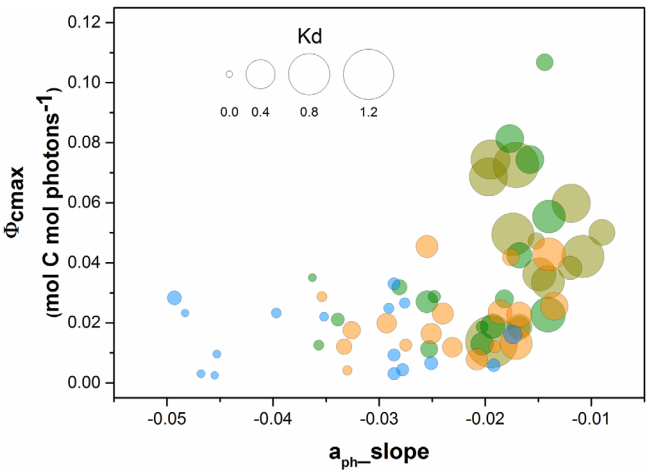

Figure 6. Relationship between the quantum yield of photosynthetic carbon fixation and the photoacclimation index (a_{ph}_slope) as a function of K_d (indicated by symbol size) and geographic zone (symbol color as in Figure 5).

also explain the negative correlation between Φ_{cmax} and temperature (Table 2). Therefore, it can be concluded that diatom-dominant populations possessed higher light utilization efficiency for photosynthesis and that observed differences in Φ_{cmax} reflect a variety of differences related to community and pigment composition and environmental variables.

We observed a significant relationship between Φ_{cmax} and a_{ph}_slope (Table 2), which was consistent with photoacclimation as an additional factor influencing variations in Φ_{cmax}. The a_{ph}_slope decreased (increase in negative values) from the low-light delta to high-light environments of far field and offshore (Figure 6). The decrease in Φ_{cmax} in the far-field and offshore zones could be due the increase in PPC:PSC, and a_{ph}_slope is inversely proportional to PPC:PSC ratio (mentioned earlier). Key factors influencing the variability in Φ_{cmax} include relative abundance of nonphotosynthetic pigments, the number of functional reaction centers, and/or the cyclic electron flow around photosystem I or II [*Babin et al.*, 1996]. A study in North Atlantic has also shown significant negative relationships between Φ_{cmax} and $a_{ph}(440)$:$a_{ph}(676)$ and to the ratio of nonphotosynthetic pigments to chl *a* concentrations [*Stuart et al.*, 2000]. High values of PPC are generally found in high irradiance-acclimated cells [*Morel and Bricaud*, 1981]. In our study, we surmised that the significant relationship observed between Φ_{cmax} and a_{ph}_slope was a consequence of phytoplankton assemblages acclimating to ambient light by regulating the relative amounts of photosynthetic or nonphotosynthetic pigments. This would, in turn, influence the phytoplankton absorption spectra and thereby the pattern of variation in Φ_{cmax}. Phytoplankton acclimated to low-light conditions tend to have lower P^B_{max} and E_k than in regions with high light. The PPC group of pigments mainly functions by dissipating the absorbed energy as heat under high-light conditions and so plays a photoprotective role in the cell [*Falkowski and Raven*, 1997].

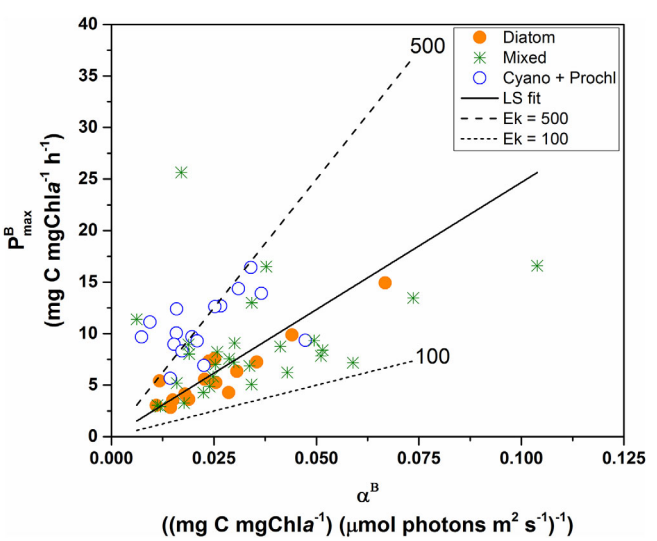

Figure 7. Relationship between light-saturated photosynthetic rate, P^B_{max}, and the light-limited slope, α^B, categorized by dominant (>60%) phytoplankton group. The dashed lines are the E_k (μmol photons m^{-2} s^{-1}) = P^B_{max}/α^B.

In contrast to some previous studies [*Zhao and Quigg*, 2015; *Lohrenz et al.*, 1994], a strong covariance in P^B_{max} and α^B was found in this study. The strong positive covariation between P^B_{max} and α^B (Figure 7) is typical of E_k-independent variability that has been frequently observed in other ocean regions [*Behrenfeld et al.*, 2004, and references therein]. However, the underlying basis for the E_k-independent variability remains largely unresolved. This covariation has been linked to the diversion of reductants produced by the light reactions of photosynthesis to reactions other than carbon fixation. Among potential causes for this diversion of reductants is nutrient limitation [e.g., *Côté and Platt*, 1983; *Behrenfeld et al.*, 2004]. A

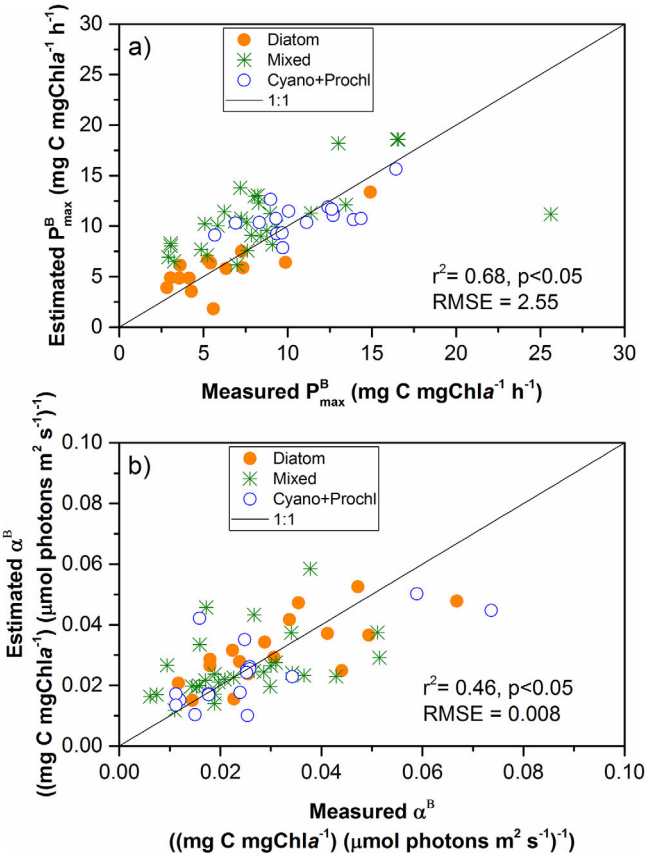

Figure 8. Multiple linear regression estimates of (a) P^B_{max} and (b) α^B in comparison to observed values. Coefficients for the regression are given in Tables 3a and 3b.

recent study [*John et al.*, 2012] in the Mississippi River plume observed E_k-independent variability in the larger fraction (>2µm) of phytoplankton and suggested nutrient-related stress probably resulted in the E_k-independent variability in those groups. The P^B_{max} and α^B relationship observed in our study (Figure 7) was associated with differences between the diatom-dominated and cyano + prochl-dominated groups of phytoplankton. Therefore, an alternative explanation for the P^B_{max} and α^B relationship is that it reflects underlying differences in the photometabolism of photosynthetic prokaryotes and eukaryotes (e.g., diatoms and the mixed group) [*Behrenfeld et al.*, 2004].

4.2. Estimation of P-E Parameters: Implication for Primary Production Estimates in NGOM

An examination of differences in P^B_{max} and α^B for each phytoplankton group did not reveal significant differences between the different geographic regions. There were significant differences in parameters between the phytoplankton groups, however. Hence, we sought to develop empirical relationships of P-E properties to optical indices of phytoplankton absorption and environmental variables that were specific to each subset of stations dominated by the different phytoplankton groups for the entire study area. We used a stepwise multiple-regression model with the predictor variables listed in Table 3a to develop a relationship to estimate P-E parameters. For all data, the stepwise multiple regression explained >60% of the variation for P^B_{max} and ~46% for α^B (Figure 8). Temperature, a_{ph}(676), a_{ph}_slope, and a_{ph}(440):a_{ph}(676) were the best predictors for P^B_{max}, while DIN, a_{ph}(676), and a_{ph}(440):a_{ph}(676) were best predictors for α^B. Using the combination of environmental variables and phytoplankton group-specific indices to estimate P-E parameters, we obtained a mean absolute percent error for the estimate of P^B_{max} was 26.9% (Figure 8a) and $\alpha^B$was 15.4% (Figure 8b). The percent root-mean-square error (RMSE) of model estimates was generally low; however, larger errors were associated with the mixed phytoplankton-dominated stations. The maximum error and large variability observed in the mixed groups likely reflects the photophysiological differences among taxa within the mixed community.

The idea of using phytoplankton class-specific indices to improve estimates of P-E parameters has been previously implemented by *Uitz et al.* [2008], and the results of this study provide further support for such an approach. The predictor values of a_{ph}(676), a_{ph}_slope, and a_{ph}(440):a_{ph}(676) can be acquired or derived on synoptic scales through satellite ocean color imagery, and may be used to refine estimates of P^B_{max} (and α^B) in the NGOM region. Accounting for variations in phytoplankton community composition should in principle allow for improved modeling of primary production for the river-influenced continental margin of the NGOM as well as other systems in which there are substantial, spatial gradients in phytoplankton community composition.

5. Conclusions

This study characterized the photophysiological and bio-optical properties of the phytoplankton community in different geographical zones (light and nutrient regimes, physicochemical conditions) of the NGOM.

Our results highlight the importance of phytoplankton community composition and associated optical properties as key factors in explaining the variability of P-E curve parameters in the dynamic-complex continental margin of NGOM. Photoacclimation of phytoplankton in different light environments, including delta, intermediate, far field, and offshore, was evident and considered to be a factor regulating the efficiency of carbon fixation in photosynthesis (quantum yield). Our findings were unprecedented in revealing significant differences in photosynthetic parameters between the major phytoplankton groups in northern Gulf of Mexico waters. This enabled us to build an empirical model based on multiple linear regression for the major phytoplankton groups across the entire study area. The empirical model presented in this study, specific for subsets of stations dominated by different phytoplankton groups, generated satisfactory estimates of the P^B_{max} (and α^B). These findings are encouraging for further efforts to apply this approach for wider-scale modeling of primary production.

Acknowledgments

We thank the captain and crews of R/V *Cape Hatteras* and R/V *Hugh R. Sharp* for their support. We are grateful for funding support from the National Science Foundation (OCE-0752254) and the National Aeronautics and Space Administration (NNX10AU06G, NNX12AP84G, and NNX14AO73G). We are grateful to the two anonymous reviewers for their valuable suggestions in improving this paper. We also thank S. R. Wright and H. Higgins graciously provided the CHEMTAX (v 1.95) software. The data used are listed in the references, tables, supplements, and in the NASA SeaBASS data archive (http://seabass.gsfc.nasa.gov/seabasscgi/archive.cgi?q=/UMASS_D).

References

Babin, M., A. Morel, H. Claustre, A. Bricaud, Z. Kolber, and P. G. Falkowski (1996), Nitrogen- and irradiance-dependent variations of the maximum quantum yield of carbon fixation in eutrophic, mesotrophic and oligotrophic marine systems, *Deep Sea Res., Part I*, *43*(8), 1241–1272.

Babin, M., D. Stramski, G. M. Ferrari, H. Claustre, A. Bricaud, G. Obolensky, and N. Hoepffner (2003), Variations in the light absorption coefficients of phytoplankton, nonalgal particles, and dissolved organic matter in coastal waters around Europe, *J. Geophys. Res.*, *108*(C7), 3211, doi:10.1029/2001JC000882.

Bannister, T. T. (1974), Production equations in terms of chlorophyll concentration, quantum yield, and upper limit to production, *Limnol. Oceanogr.*, *19*(1), 1–12.

Behrenfeld, M. J., E. Marañón, D. A. Siegel, and S. B. Hooker (2002), Photoacclimation and nutrient-based model of light-saturated photosynthesis for quantifying oceanic primary production, *Mar. Ecol. Prog. Ser.*, *228*, 103–117.

Behrenfeld, M. J., O. Prasil, M. Babin, and F. Bruyant (2004), In search of a physiological basis for covariations in light-limited and light saturated photosynthesis, *J. Phycol.*, *40*(1), 4–25.

Bouman, H., T. Platt, S. Sathyendranath, and V. Stuart (2005), Dependence of light-saturated photosynthesis on temperature and community structure, *Deep Sea Res., Part I*, *52*(7), 1284–1299.

Bricaud, A., and D. Stramski (1990), Spectral absorption coefficients of living phytoplankton and nonalgal biogenous matter: A comparison between the Peru upwelling area and the Sargasso Sea, *Limnol. Oceanogr.*, *35*(3), 562–582.

Bricaud, A., H. Claustre, J. Ras, and K. Oubelkheir (2004), Natural variability of phytoplanktonic absorption in oceanic waters: Influence of the size structure of algal populations, *J. Geophys. Res.*, *109*, C11010, doi:10.1029/2004JC002419.

Campbell, J. W. (1995), The lognormal distribution as a model for bio-optical variability in the sea, *J. Geophys. Res.*, *100*, 13,237–13,254.

Cermeno, P., E. Maranno, J. Rodriguez, and E. Fernandez (2005), Large-sized phytoplankton sustain higher carbon-specific photosynthesis than smaller cells in a coastal eutrophic ecosystem, *Mar. Ecol. Prog. Ser.*, *297*, 51–60.

Chakraborty, S. (2013), Phytoplankton community distribution and light absorption properties in the northern Gulf of Mexico, PhD thesis, Univ. of South. Miss., Hattiesburg, Miss.

Chakraborty, S., and S. E. Lohrenz (2015), Phytoplankton community structure in the river influenced continental margin of the northern Gulf of Mexico, *Mar. Ecol. Prog. Ser.*, *521*, 31–47.

Claustre, H., M. Babin, D. Merien, J. Ras, L. Prieur, S. Dallot, O. Prasil, H. Dousova, and T. Moutin (2005), Toward a taxon-specific parameterization of bio-optical models of primary production: A case study in the North Atlantic, *J. Geophys. Res.*, *110*, C07S12, doi:10.1029/2004JC002634.

Côté, B., and T. Platt (1983), Day-to-day variations in the spring-summer photosynthetic parameters of coastal marine phytoplankton, *Limnol. Oceanogr.*, *28*(2), 320–344.

Dagg, M. J., and G. A. Breed (2003), Biological effects of Mississippi River nitrogen on the northern Gulf of Mexico—A review and synthesis, *J. Mar. Syst.*, *43*(3–4), 133–152.

Davison, I. R. (1991), Environmental effects on algal photosynthesis: Temperature, *J. Phycol.*, *27*(1), 2–8, doi:10.1111/j.0022-3646.1991.00002.x.

De Vargas, C., et al. (2015), Eukaryotic plankton diversity in the sunlit ocean, *Science*, *348*(6237), 1261605.

Dortch, Q., and T. E. Whitledge (1992), Does nitrogen or silicon limit phytoplankton production in the Mississippi River plume and nearby regions?, *Cont. Shelf Res.*, *12*(11), 1293–1309.

D'Sa, E. J., and S. F. DiMarco (2009), Seasonal variability and controls on chromophoric dissolved organic matter in a large river-dominated coastal margin, *Limnol. Oceanogr.*, *54*(6), 2233–2242.

D'Sa, E. J., R. L. Miller, and B. A. McKee (2007), Suspended particulate matter dynamics in coastal waters from ocean color: Application to the northern Gulf of Mexico, *Geophys. Res. Lett.*, *34*, L23611, doi:10.1029/2007GL031192.

Eisner, L. B., M. S. Twardowski, T. J. Cowles, and M. J. Perry (2003), Resolving phytoplankton photoprotective:photosynthetic carotenoid ratios on fine scales using in situ spectral absorption measurements, *Limnol. Oceanogr.*, *48*(2), 632–646.

Falkowski, P. G., and J. A. Raven (1997), *Aquatic Photosynthesis*, Blackwell Sci., Malden, Mass.

Feng, Y., S. F. DiMarco, and G. A. Jackson (2012), Relative role of wind forcing and riverine nutrient input on the extent of hypoxia in the northern Gulf of Mexico, *Geophys. Res. Lett.*, *39*, L09601, doi:10.1029/2012GL051192.

Fennel, K., R. Hetland, Y. Feng, and S. Dimarco (2011), A coupled physical-biological model of the northern Gulf of Mexico shelf: Model description, validation and analysis of phytoplankton variability, *Biogeosciences*, *8*(7), 1881–1899.

Fujuta, Y., A. Murakami, A. Katunori, and K. Ohki (1994), Short-term and long-term adaptation of the photosynthetic apparatus: Homeostatic properties of thylakoids, in *The Molecular Biology of Cyanobacteria*, edited by D. A. Bryant, pp. 677–692, Kluwer Acad., Dorecht, Netherlands.

Harrison, W. G., and T. Platt (1986), Photosynthesis-irradiance relationships in polar and temperate phytoplankton populations, *Polar Biol.*, *5*, 153, doi:10.1007/BF00441695.

Hashimoto, S., and A. Shiomoto (2002), Light utilization efficiency of size-fractionated phytoplankton in the subarctic Pacific, spring and summer 1999: High efficiency of large-sized diatom, *J. Plankton Res.*, *24*(1), 83–87.

Heilman, S., and N. N. Rabalais (2008), Gulf of Mexico LME, in *A Perspective on the Changing Conditions in LME of the World's Regional Seas, UNEP Reg. Seas Rep. Stud., 182*, edited by K. Sherman and G. Hempel, pp. 673–688, U. N. Environ. Program, Nairobi.

Huang, W.-J., W.-J. Cai, R. M. Castelao, Y. Wang, and S. E. Lohrenz (2013), Effects of a wind-driven cross-shelf large river plume on biological production and CO_2 uptake on the Gulf of Mexico during spring, *Limnol. Oceanogr.*, *58*(5), 1727–1735.

John, D. E., J. M. López-Díaz, A. Cabrera, N. A. Santiago, J. E. Corredor, D. A. Bronk, and J. H. Paul (2012), A day in the life in the dynamic marine environment: how nutrients shape diel patterns of phytoplankton photosynthesis and carbon fixation gene expression in the Mississippi and Orinoco River plumes, *Hydrobiologia*, *679*(1), 155–173.

Justic, D., N. N. Rabalais, R. E. Turner, and Q. Dortch (1995), Changes in nutrient structure of river-dominated coastal waters: Stoichiometric nutrient balance and its consequences, *Estuarine Coastal Shelf Sci.*, *40*(3), 339.

Laurent, A., K. Fennel, J. Hu, and R. Hetland (2012), Simulating the effects of phosphorus limitation in the Mississippi and Atchafalaya River plumes, *Biogeosciences*, *9*(11), 4707–4723, doi:10.5194/bg-9-4707-2012.

Lehrter, J. C., M. C. Murrell, and J. C. Kurtz (2009), Interactions between freshwater input, light, and phytoplankton dynamics on the Louisiana continental shelf, *Cont. Shelf Res.*, *29*(15), 1861–1872.

Lehrter, J. C., D. S. Ko, M. C. Murrell, J. D. Hagy, B. A. Schaeffer, R. M. Greene, R. W. Gould, and B. Penta (2013), Nutrient distributions, transports, and budgets on the inner margin of a river-dominated continental shelf, *J. Geophys. Res. Oceans*, *118*, 4822–4838, doi:10.1002/jgrc.20362.

Lewis, M., and J. C. Smith (1983), A small volume, short-incubation-time method for measurement of photosynthesis as a function of incident irradiance, *Mar. Ecol. Prog. Ser.*, *13*, 99–102.

Liu, H., I. Probert, J. Uitz, H. Claustre, S. Aris-Brosou, M. Frada, F. Not, and C. de Vargas (2009), Extreme diversity in noncalcifying haptophytes explains a major pigment paradox in open oceans, *Proc. Natl. Acad. Sci. U. S. A.*, *106*(31), 12,803–12,808.

Lohrenz, S., G. Fahnenstiel, and D. Redalje (1994), Spatial and temporal variations of photosynthetic parameters in relation to environmental conditions in coastal waters of the northern Gulf of Mexico, *Estuaries*, *17*(4), 779–795.

Lohrenz, S., D. Wiesenburg, R. Arnone, and X. Chen (1999), What controls primary production in the Gulf of Mexico?, in *The Gulf of Mexico Large Marine Ecosystem: Assessment, Sustainability and Management*, edited by H. Kumpf, K. A. Steidinger, and K. Sherman, pp. 151–170, Blackwell Sci., Malden, Mass.

Lohrenz, S. E. (2000), A novel theoretical approach to correct for pathlength amplification and variable sampling loading in measurements of particulate spectral absorption by the quantitative filter technique, *J. Plankton Res.*, *22*(4), 639–657.

Lohrenz, S. E., A. D. Weidemann, and M. Tuel (2003), Phytoplankton spectral absorption as influenced by community size structure and pigment composition, *J. Plankton Res.*, *25*(1), 35–61.

Lohrenz, S. E., D. G. Redalje, W.-J. Cai, J. Acker, and M. Dagg (2008), A retrospective analysis of nutrients and phytoplankton productivity in the Mississippi River plume, *Cont. Shelf Res.*, *28*(12), 1466–1475.

Lohrenz, S. E., S. Chakraborty, M. Huettel, J. Herrerra Silveria, K. Gundersen, D. Redalje, J. Wiggert, B. E. Denton, and J. Lehrter (2014), Primary production, in *Report of the U.S. Gulf of Mexico Carbon Cycle Synthesis Workshop*, edited by H. M. Benway and P.G. Coble, pp. 28–38, Ocean Carbon and Biogeochem. Program and North Am. Carbon Program.

MacIntyre, H. L., and R. J. Geider (1996), Regulation of Rubisco activity and its potential effect on photosynthesis during mixing in a turbid estuary, *Mar. Ecol. Prog. Ser.*, *144*, 247–264.

MacIntyre, H. L., T. M. Kana, T. Anning, and R. J. Geider (2002), Photoacclimation of photosynthesis irradiance response curves and photosynthetic pigments in microalgae and cyanobacteria, *J. Phycol.*, *38*(1), 17–38.

Mackey, M. D., D. J. Mackey, H. W. Higgins, and S. W. Wright (1996), CHEMTAX—A program for estimating class abundances from chemical markers: Application to HPLC measurements of phytoplankton, *Mar. Ecol. Prog. Ser.*, *144*(1–3), 265–283.

Malone, T. C., and P. J. Neale (1981), Parameters of light-dependent photosynthesis for phytoplankton size fractions in temperate estuarine and coastal environments, *Mar. Biol.*, *61*(4), 289–297.

Marra, J., C. C. Trees, and J. E. O'Reilly (2007), Phytoplankton pigment absorption: A strong predictor of primary productivity in the surface ocean, *Deep Sea Res., Part I*, *54*, 155–163.

Mitchell, B. G., and O. Holm-Hansen (1991), Observations of modeling of the Antarctic phytoplankton crop in relation to mixing depth, *Deep Sea Res., Part A*, *38*(8–9), 981–1007.

Mitchell-Innes, B. A., and D. R. Walker (1991), Short-term variability during an anchor station study in the southern Benguela upwelling system: Phytoplankton production and biomass in relation to species changes, *Prog. Oceanogr.*, *28*(1), 65–89.

Morel, A., and A. Bricaud (1981), Theoretical results concerning light absorption in a discrete medium, and application to specific absorption of phytoplankton, *Deep Sea Res., Part A*, *28*(11), 1375–1393.

Platt, T., C. L. Gallegos, and W. G. Harrison (1980), Photoinhibition of photosynthesis in natural assemblages of marine phytoplankton, *J. Mar. Res.*, *38*, 687–701.

Platt, T., H. Bouman, E. Devred, C. Fuentes-Yaco, and S. Sathyendranath (2005), Physical forcing and phytoplankton distributions, *Sci. Mar.*, *69*, suppl. 1, 55–73.

Quigg, A., J. Sylvan, A. Gustafson, T. Fisher, R. Oliver, S. Tozzi, and J. Ammerman (2011), Going west: Nutrient limitation of primary production in the northern Gulf of Mexico and the importance of the Atchafalaya River, *Aquat. Geochem.*, *17*(4–5), 519–544.

Raven, J. A. and R. J. Geider (1988), Temperature and algal growth, *New Phytol.*, *110*(4), 441–461.

Ren, S. (2010), Molecular detection of marine N_2 fixation by cyanobacteria in the northern Gulf of Mexico, master's thesis, Univ. South. Miss., Hattiesburg, Miss.

Roy, S., C. A. Llewellyn, E. S. Egeland, and G. Johnsen (2011), *Phytoplankton Pigments: Characterization, Chemotaxonomy and Applications in Oceanography*, Cambridge Univ. Press, New York.

Sakshaug, E., A. Bricaud, Y. Dandonneau, P. G. Falkowski, D. A. Kiefer, L. Legendre, A. Morel, J. Parslow, and M. Takahashi (1997), Parameters of photosynthesis: Definitions, theory and interpretation of results, *J. Plankton Res.*, *19*, 1637–1670.

Sathyendranath, S., V. Stuart, B. D. Irwin, H. Maass, G. Savidge, L. Gilpin, and T. Platt (1999), Seasonal variations in bio-optical properties of phytoplankton in the Arabian Sea, *Deep Sea Res., Part II*, *46*(3–4), 633–653.

Schaeffer, B. A., G. A. Sinclair, J. C. Lehrter, M. C. Murrell, J. C. Kurtz, R. W. Gould, and D. F. Yates (2011), An analysis of diffuse light attenuation in the northern Gulf of Mexico hypoxic zone using the SeaWiFS satellite data record, *Remote Sens. Environ.*, *115*(12), 3748–3757.

Shimada, A., T. Maruyama, and S. Miyachi (1996), Vertical distribution and photosynthetic action spectre of two oceanic picophytopiancl-ters, *Prochlorococcus marinus* and *Synechococcus* sp., *Mar. Biol.*, *127*, 15, doi:10.1007/BF00993639.

Sklar, F. H., and R. E. Turner (1981), Characteristics of phytoplankton production off Barataria Bay in an area influenced by the Mississippi River, *Contrib. Mar. Sci.*, *24*, 93–106.

Stramski, D., and A. Morel (1990), Optical properties of photosynthetic picoplankton in different physiological states as affected by growth irradiance, *Deep Sea Res., Part A*, *37*(2), 245–266.
Stramski, D., A. Bricaud, and A. Morel (2001), Modeling the inherent optical properties of the ocean based on the detailed composition of the planktonic community, *Appl. Opt.*, *40*(18), 2929–2945.
Stuart, V., S. Sathyendranath, E. J. H. Head, T. Platt, B. Irwin, and H. Maass (2000), Bio-optical characteristics of diatom and prymnesiophyte populations in the Labrador Sea, *Mar. Ecol. Prog. Ser.*, *201*, 91–106.
Suggett, D. J., C. M. Moore, A. E. Hickman, and R. J. Geider (2009), Interpretation of fast repetition rate (FRR) fluorescence: Signatures of phytoplankton community structure versus physiological state, *Mar. Ecol. Prog. Ser.*, *376*, 1–19.
Sukenik, A., J. Bennett, and P. Falkowski (1987), Light-saturated photosynthesis—Limitation by electron transport or carbon fixation?, *Biochim. Biophys. Acta Bioenergetics*, *891*(3), 205–215.
Turner, R. E., N. N. Rabalais, R. B. Alexander, G. McIsaac, and R. W. Howarth (2007), Characterization of nutrient, organic carbon, and sediment loads and concentrations from the Mississippi River into the northern Gulf of Mexico, *Estuaries Coasts*, *30*(5), 773–790.
Twardowski, M. S., E. Boss, J. M. Sullivan, and P. L. Donaghay (2004), Modeling the spectral shape of absorption by chromophoric dissolved organic matter, *Mar. Chem.*, *89*, 69–88.
Uitz, J., Y. Huot, F. Bruyant, M. Babin, and H. Claustre (2008), Relating phytoplankton photophysiological properties to community structure on large scales, *Limnol. Oceanogr.*, *53*(2), 614–630.
Uitz, J., H. Claustre, B. Gentili, and D. Stramski (2010), Phytoplankton class-specific primary production in the world's oceans: Seasonal and interannual variability from satellite observations, *Global Biogeochem. Cycles*, *24*, GB3016, doi:10.1029/2009GB003680.
Wawrik, B., and J. H. Paul (2004), Phytoplankton community structure and productivity along the axis of the Mississippi River plume in oligotrophic Gulf of Mexico waters, *Aquat. Microbial Ecol.*, *35*(2), 185–196.
Xie, Y., B. Huang, L. Lin, E. A. Laws, L. Wang, S. Shang, T. Zhang, and M. Dai (2015), Photosynthetic parameters in the northern South China Sea in relation to phytoplankton community structure, *J. Geophys. Res. Oceans*, *120*, 4187–4204, doi:10.1002/2014JC010415.
Xue, Z., R. He, K. Fennel, W. J. Cai, S. Lohrenz, and C. Hopkinson (2013), Modeling ocean circulation and biogeochemical variability in the Gulf of Mexico, *Biogeosciences*, *10*(11), 7219–7234.
Zhao, Y., and A. Quigg (2015), Study of photosynthetic productivity in the northern Gulf of Mexico: Importance of diel cycles and light penetration, *Cont. Shelf Res.*, *102*, 33–46.